International Journal of Engineering

Utilization of Gene Expression Programming for Modeling of Mechanical Performance of Titanium/Carbonated Hydroxyapatite Nanobiocomposites: The Combination of Artificial Intelligence and Material Science

M. R. Shojaei[a], G. R. Khayati*[b], A. Hasani[a]

[a] Department of Materials Science and Engineering, Sharif University of Technology, Tehran, Iran
[b] Department of materials science and Engineering, Shahid Bahonar University of Kerman, Kerman, Iran

P A P E R I N F O	*A B S T R A C T*
	Titanium carbonated hydroxyapatite (Ti/CHA) nanobiocomposites have extensive biological applications due to the excellent biocompatibility and similar characteristics to the human bone. Ti/CHA nanobiocomposite has good biological properties but it suffer from diverse characteristics especially in hardness, Young's modulus, apparent porosity and relative density. This investigation is an attempt to propose the predictive models using gene expression programming (GEP) to estimate these characteristics. In this regards, GEP is used to model and compare the effect of practical variables including pressure, Ti/CHA contents and sintering temperature on their monitored properties. To achieve this goal, 90 different experiments were considered to create the GEP models. Selected data set were divided randomly into 63 training sets and 27 testing sets. Finally, five of the best models were reported for each different output. Sensitivity analyses were done to determine and rank the practical parameters on each of the investigated properties and revealed that wt.% Ti, wt.% CHA, compaction pressure (MPa) and temperature ($^{\circ}$C), respectively are the most effective parameters on hardness, Young's modulus, shear modulus, apparent porosity and relative density. By comparing the results, a very good agreement was observed between the experimental data and the results obtained from GEP model.

NOMENCLATURE

Wt.% CHA	Weight percent of carbonated hydroxyapatite	R^2	Correlation coefficient
Wt.% Ti	Weight percent of titanium	RMSE	Root mean square error
GEP	gene expression programming	RRSE	Root relative squared error
PSO	particles swarm optimization	MAPE	Mean absolute percentage error
T	Reaction temperature ($^{\circ}$C)	N (= 90)	Number of datasets used in the testing and training phases
P	Compaction pressure (MPa)	t_i	The measured values by models
E	Elastic module (Gpa)	p_i	The predicted values by models

1. INTRODUCTION

It is well known that about 65 wt.% of bone is made of Hydroxyapatite ($Ca_{10}(PO_4)_6(OH)_2$, which is one of the most commonly biocompatible and nontoxic ceramics with the similar chemical and structural characteristics to the human natural bone [1-3]. Therefore, HA is extensively applied for repair and reconstruction of bone tissue defects, making dental, orthopedics and middle ear implants [4, 5], drug delivery and gene delivery [6]. Unfortunately, HA have some disadvantages such as: i. Bone grafting ability of the HA is very slow; ii. The implant is not safe from bacteria; iii. The rate of degradation of this material is slower than the rate of osteogenesis; and iv. The mechanical properties of HA are weaker than living bone [7, 8]. To solve monitored

*Corresponding Author Institutional Email: Khayatireza@gmail.com (G. R. Khayati)

problems (CO_3^{-2}) added to HA. It is clear that except for calcium and phosphorus ions, carbonate ions also in the natural bone mineral, and carbonate ions make up 2 to 8% of the inorganic composition of bone [5]. Therefore, carbonated hydroxyapatite (CHA) has a very similar composition to the human bone. Also, CHA has better solubility and higher biological activity than HA [9-11]. Another way to improve the mechanical properties is the manufacture of nanobiocomposites with some group of metals such as Ti which can be the best choice for the production of CHA nanocomposites due to its unique properties such as relatively low modulus, low density, high strength, corrosion resistance and biocompatibility. However, poor tribological properties, unfavorable mechanical properties, and inability to regenerate bone tissue are the most important disadvantages of Ti [12]. It is noteworthy that CHA and Ti have the ability to compensate for each other's shortcomings and defects, so that combination of these constituents produce a nanocomposite with desirable properties for medical applications. There are various approaches for the preparation of these nanocomposites including sol-gel, co-precipitation, and mechanochemical routes. Among these, the ease of chemical-chemical reduction, high speed, relatively low operating costs, process at the ambient temperature has made it a suitable candidate for the preparation of the composite in this study [13, 14].

Artificial intelligence (AI) based methods such as artificial neural network (ANN), gene expression programming (GEP), and molecular dynamics simulation have been used in many fields, including engineering in recent years [15-17]. For example, GEP has been used extensively in the production of nanocomposites by mechanical alloying method to predict hardness and minimize sintering time [18, 19]. Side by side comparison of literature about the modeling of preparation method are abbreviated in Table 1. To the best of our knowledge, the GEP molding has not been used to optimize the parameters affecting the mechanical properties of Ti/CHA nanocomposites until now. Accordingly, the main contributions of this study are: (a)

the usage of GEP to model the consolidation process of preparation of Ti/CHA nanocomposite by mechanochemical approach; (b) assessment of the effect of input parameters such as sintering temperature, Ti and CHA contents on hardness, Young's modulus, apparent porosity, relative density, and theoretical density of the Ti-CHA nanocomposite and (c) the determination and rank of the effect of each practical variable on selected characteristics.

2. OPTIMAZATION APPROACH

This section describes the gene expression programming as a basic concept that is essential to this study.

2. 1. Gene Expression Programming   Gene expression programming (GEP), introduced by Ferreira [20] is a new population based evolutionary algorithm that can overcome the disadvantages and limitations of genetic algorithm (GA) and genetic programming (GP) [21]. The GEP encodes the individuals of the created computer programs as linear strings of fixed size (the genome or chromosomes) which are afterwards expressed as nonlinear entities with different sizes and shapes. These entities called as expression trees (ET). Usually these individuals are made up of only one chromosome and each chromosome can have one or more genes. Genes have two main parts: the head and the tail. The head consists of some mathematical operators, variables and constants ($*$, $/$, $+$, $-$, $\sqrt{}$, sin, cos, 1, a, b, c) which are used to encode a mathematical expression [18, 19]. The tail just consists of variables and constants (1, a, b, c), which are called terminal symbols. Accordingly, two different languages (Karva Language) are utilized in GEP: the language of the genes and the language of ETs [22]. The translation of Karva to the ET initiates from the leading position in the ET and continues through the string. ET can be translated into the K-expression by registration of the nodes from root layer to the deepest layer [23, 24]. Genes are joined by the linking functions "addition", "subtraction", "multiplication" and "division". For example, an algebraic expression [(($a*b$)-

TABLE 1. Side by side comparison of literatures about the modeling of preparation of nanocomposite by consolidation of prepared powder by mechanochemical approach

No.	model	Output parameters						Year, [Ref.]
		Compressive strength (MPa)	Porosity (%)	Size of nanoparticle	Hardness(Gpa)	E (Gpa)	Relative density (%)	
1	GEP			✓				[21]
2	PSO			✓				[19]
3	GEP	✓	✓					[16]
4	GEP		✓		✓	✓	✓	This study

c) + √(d-e)] can be shown by a 2 gene chromosome or an expression tree [25]. Figure 1 represents how a chromosome with two genes is encoded as a linear string and how it is expressed as an ET.

3. EXPERIMENTAL METHOD

3. 1. Synthesis and Characterization of Ti-CHA Nanocomposite
Ti powders (Merck, 99 wt.%) with the average particle size 30 mm and CHA were used as mother materials to produce Ti-CHA nanocomposite in various ratios (Table 2) using mechanical alloying. Firstly, the as-received powders of Ti and CHA were mechanically blended in Ar atmosphere using SPEX 8000 for 12 h with the ball-to-powder ratio equal to 1:2 until a good distribution was achieved. The diameter of balls were 10 mm. Secondly, the powders obtained in step 1 were milled for 10 h in a planetary ball mill with rotational speed equal to 400 rpm and ball-to-powder ratio equal to 20:1. Thirdly, the powder was pressed at the pressure of 50 MPa and 80 MPa. After that, the green compacts were sintered at temperatures listed in Table 2.

The apparent porosity of sintered samples was measured by the Archimedes' method using distilled water (ASTM: B962-13) for different temperatures, i.e. 800, 900, 1100 and 1300 °C. To calculate the theoretical density of sintered samples, first relative density was calculated using the measured bulk density (with dense values of Ti and HA as 4.506 and 3.156 g/cm^3, respectively) and then theoretical density was determined for each samples. The Vickers hardness of samples was measured under the load of 10 N for 20 sec. The Lame's constants, i.e. λ and μ were measured by pulse-echo technique MATEC Model MBS8000 DSP (ultrasonic digital signal processing) system with 5 MHz resonating at room temperature. Then, the values of the Young's modulus (E) was calculated from Equations (1)-(3):

$$\lambda = \rho\left(V_L^2 - 2V_S^2\right) \tag{1}$$

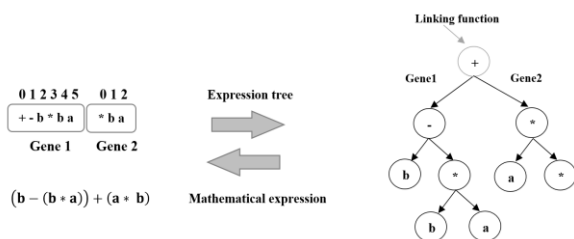$$\mu = \rho V_S^2 \tag{2}$$

Figure 1. Translating ET language to the mathematical formula [25]

TABLE 2. The details of experimental data for the developed GEP model

Inputs	Variables (Max, Min)
wt.% Ti	24-100
wt.% CHA	0-76
Compaction pressure (MPa)	50-80
Temperature (ºC)	800-1200
Output	*
Apparent porosity, %	5.96-8.95
E (GPa)	108.52-143.1
Hardness (GPa)	2.26-2.99
Relative density (%)	88.47-93.23
Theoretical density (g/cm^3)	4.233-4.325

$$E = \mu\frac{3\lambda + 2\mu}{\lambda + \mu} \tag{3}$$

where, V_l^2 and V_s^2 are longitudinal and shear ultrasonic velocities, respectively. p is the material bulk density.

3. 2. The Modelling Method
The main parameters of GEP are terminal set, termination condition, fitness function, control parameters and function set [21]. Figure 2 represents the schematic of the GEP algorithm. The process begins with the creation of chromosomes of fixed length for all individuals, randomly. Afterwards, the chromosomes are expressed and the fitness of each individual is investigated. Following to that, the best-fit individuals are chosen to apply the reproduction. The process continues with the new individual for a number of generations until a best solution is found. The genetic operations, e.g. mutation, cross over and reproduction are carried out for the conversion in population [26].

GeneXproTools 5.0 software was used to establish the relationship between input and output parameters, including hardness, elastic modulus, apparent porosity, relative density and theoretical density. In this study, a large number of chromosomes were tested to find the models with the least error. According to the author's information, GEP has been used to investigate the effect of inputs on several metallurgical outputs, which are listed in Table 2. The ranges of parameters involved in the GEP predictive algorithm in this study are summarized in Table 3. To optimize the practical parameters, this study proposes an optimization process using the GEP algorithm.

The performance of the GEP model depends on the number of chromosomes, head sizes, number of genes, linking function, fitness function, mutation, inversion,
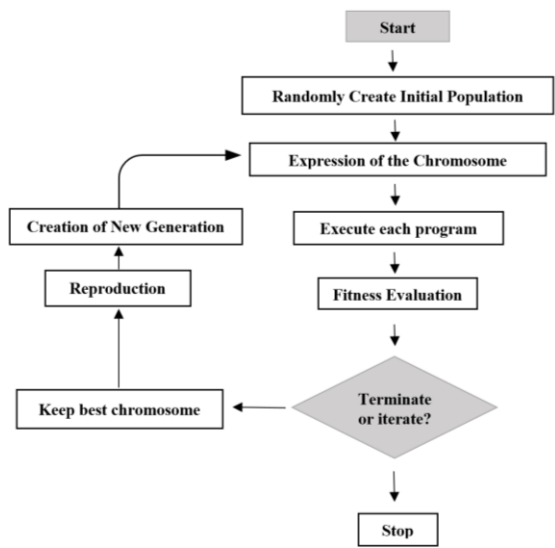
Figure 2. A fundamental flowchart of the GEP algorithm

TABLE 3. GEP parameters settings for the proposed model

GEP parameters definition	Settings
Number of chromosomes	26-30
Head size	8-10
Number of genes	8
Linking function	Multiplication/Division
Fitness function error type	RRSE
Constant per gene	1
Mutation rate	0.0044
Inversion rate	0.15
One point recombination rate	0.2
Two point recombination rate	0.2
Gene recombination rate	0.1
Gene transposition rate	0.1

transposition, constants per gene, number of involving operators, and lower and upper bounds [27]. Table 3 illustrates the features of each model. GEP 1 to GEP 5 models are the most optimal for respectively outputs including hardness, elastic modules, apparent porosity, relative density and theoretical density. The number of functions were changed between 4-17 and in the whole models, the basic operators $(+, -, \times$ and $/)$ were presented constantly while the others Sqrt, 3Rt, Exp, Sin, Cos, Atan, Tan, x^2 , x^3 and Ln Csc, Sec, Cot Tanh, Inv, Max^2, Min^2, Avg$^2)$ were added when needed.

4. RESULTS AND DISCUSSION

4. 1. Modelling Observations
To investigate the

capabilities of the GEP-based formulation in this study, several statistical parameters were used. Validation of each model by consideration of the mean absolute percentage error (MAPE), root relative square error (RRSE), mean-squared error (MSE) and R square (R^2) were used as the criteria between the experimental and predicted values according to the following Equations (4)-(7).

$$\text{MAPE} = \frac{1}{n}\sum_i \frac{|t_i - p_i|}{t_i} \times 100, \tag{4}$$

$$\text{RRSE} = \sqrt{\frac{\sum_i (t_i - p_i)^2}{\sum_i (t_i - (1/n)\sum_i t_i)^2}}, \tag{5}$$

$$\text{MSE} = \frac{1}{n}\sum_i (t_i - p_i)^2, \tag{6}$$

$$R^2 = 1 - \left(\frac{\sum_i (t_i - p_i)^2}{\sum_i (p_i)^2}\right), \tag{7}$$

Therefore, t is the experimental (target) value, p the predicted value, and n the data set number in the testing and training phases. If, R^2 values are greater than 0.7 and close to 1 and MAPE, MSE, and RRSE are close to zero, then the results obtained from the models are close to the experimental (target) results [25, 27].

To get generalization capability for the formularization, the experimental data is separated in to two sets as training and test sets. The formularizations are based on training sets and are further tested by test set values to evaluate their generalization capability [28]. All of the results predicted by the training and testing results of GEP-1 to GEP-5 model are given in Table 4. As can be seen, R^2 values for training and testing are in the range of 0.9925-0.9968 and 0.9965-0.9919, respectively, which indicates that the values predicted by GEP are close to the experimental values. The equations obtained for 5 of the best GEP models are summarized in Table 5. Equations are achieved from corresponding expression trees.

The comparison of model predictions against the experimental results of Ti/CHA nanocomposite is shown in Figure 3. It can be seen from Figure 3 that the GEP model could predict the apparent porosity, elastic moduli, hardness, relative density and theoretical density very close to the experimental values. By looking more closely at the graphs, we find that the greatest similarity between the output data and the input data is related to the elastic modulus diagram, which shows that GEP can predict the output parameters of the elastic moduli with the least possible error.

The comparison of model predictions against the experimental results of Ti/CHA nanocomposite is shown in Figure 3. It can be seen from Figure 3 that the GEP
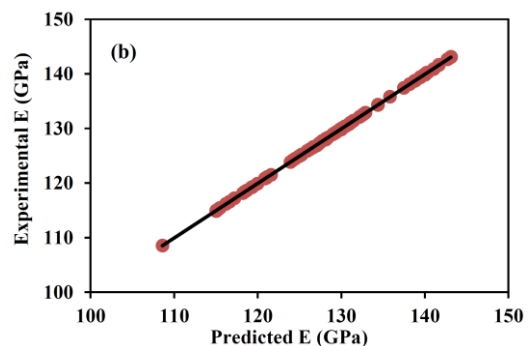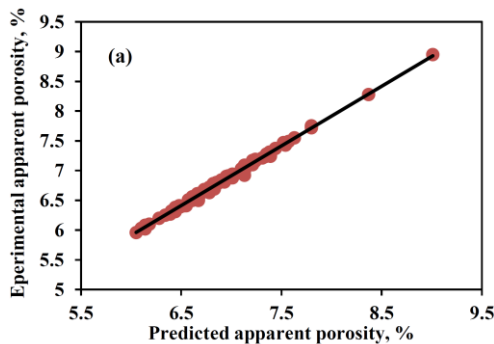
TABLE 3. Characteristics of GEP models

Model	Linking function	Head size	Number of genes	Variable used	Output parameters	Number of functions	Type of function
GEP-1	Multiplication	8	8	Wt.% Ti, Wt.% CHA, P, T	Hardness	6	+, -, *, /, X^2, Exp
GEP-2	Division	10	6	Wt.% Ti, Wt.% CHA, P, T	Elastic modules	17	+, -, *, /, X^2,Ln, Exp, 3RT, Atan, Tanh, Inv, Max^2, Min^2, Avg^2, X^3, X^5 , Sqrt
GEP-3	Division	10	8	Wt.% Ti, Wt.% CHA, P, T	Shear modules	4	+, -, *, /
GEP-4	Multiplication	8	8	Wt.% Ti, Wt.% CHA, P, T	Apparent porosity	7	+, -, *, /, X^2,Ln, Exp
GEP-5	Multiplication	9	7	Wt.% Ti, Wt.% CHA, P, T	Relative density	15	+, -, *, /, X^2,Ln, Exp, Cos, Sin, Tan, Inv, X^3, Csc, Sec, Cot

TABLE 4. Statistics of GEP models

No.	R^2		Error					
			Training			Testing		
	Training	Testing	MAPE	MSE	RRSE	MAPE	MSE	RRSE
GEP-1	0.9932	0.9965	5.9	0.0056	0.0913	3.3	0.0022	0.0832
GEP-2	0.9925	0.9941	4.6	0.0035	0.0885	4.2	0.0029	0.0891
GEP-3	0.9968	0.9919	5.08	0.0044	0.1126	4.5	0.0038	0.1022
GEP-4	0.9965	0.9949	5.5	0.0032	0.0929	9.1	0.0119	0.1129
GEP-5	0.9935	0.9932	5.6	0.0041	0.0968	5.8	0.0045	0.1067

TABLE 5. Mathematical equations for GEP model of each parameter

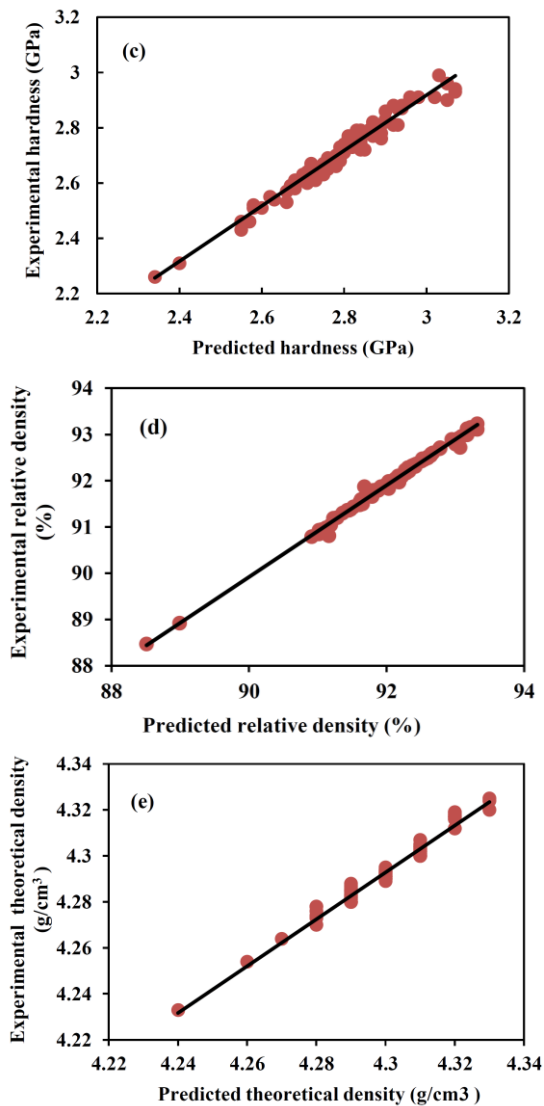| Model	Acquired equation
GEP-1	$(9.34/P) * (((0.32-P)+(exp(0.32)/(0.32*P)))^2) * (58.32* T^2)$
GEP-2	$(((log(0.7)*arctan(\%CHA))^2)+exp(log(arctan(\%Ti))))*((((\%Ti/P)*\%CHA)*(\%CHA/P))-((0.23*T)*(0.23*T))) * ((((1.0/(\%Ti))/(P+2.8))^2)*(arctan(\%CHA)-P))$
GEP-3	$(((T-\%Ti)-\%Ti)-\%CHA)-4*\%Ti / (\%CHA+(\%Ti/(((T+\%Ti)*(0.70)-(T-\%Ti)))) / ((((\%Ti)*(0.53)+(2* \%CHA)$
GEP-4	$((((P+d\%Ti)+\%Ti)-(2*T))-(exp(-25.66)+((-25.66)-\%Ti))) * log((((P*\%CHA)+(\%Ti+0.27))/((T*0.27)*log(\%CHA)))) * ((((-1.6)/(1)/((P^2+(-1.6))-(\%Ti+\%CHA)));$
GEP-5	$(0.56) * ((P+sec((0.54*P)))*cos(((1.0/(\%Ti))-0/54)) * tan((tan(cos(((reallog(T)+(-0.37))*(-0.37)))) ^2))$

Figure 3. Predicted versus experimental output parameters using GEP model, (a) Apparent porosity, (b) Elastic module, (c) Hardness, (d) Relative density, (e) Theoretical density

model could predict the apparent porosity, elastic modulus, hardness, relative density and theoretical density very close to the experimental values. By looking more closely at the graphs, we find that the greatest similarity between the output data and the input data is related to the elastic modulus diagram, which shows that GEP can predict the output parameters of the elastic modulus with the least possible error (Table 6).
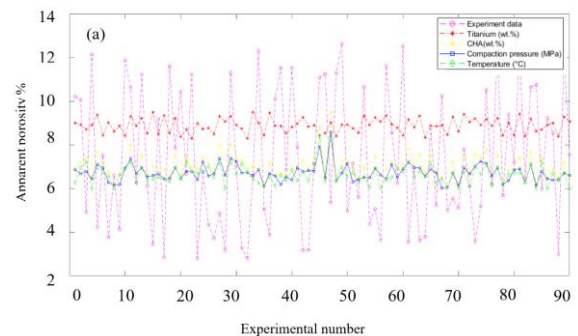
4. 3. Sensitivity Analysis   Finally, sensitivity analysis was used to investigate the effect of input parameters on the output parameters in such a way that the effect of input parameters of output parameter break

was performed by keeping the other output parameters constant. Figure 4 (a) shows the effect of input parameters on apparent porosity. As can be seen from Figure 4, the amount of Ti has the greatest effect on the porosity. In other words, porosity increases with decreasing the amount of Ti. In addition, as expected, increasing the pressure reduces the porosity. Figure 4 (b), which examines the effect of input parameters on the elastic modulus, shows that temperature has the least effect on the modulus as compared to other parameters. Examination of experimental data showed that with increasing the amount of CHA, both modulus of elasticity and hardness increase significantly and improve the properties of nanocomposite because Ti alone has good toughness but its hardness is not suitable for medical applications such as fabrication of implants and scaffold. A similar conclusion can be drawn from the graphs related to sensitivity analysis.

In Figures 4 (c, d, e), which are related to the study of the effect of input parameters on the output parameters of hardness, relative density and theoretical density, respectively, it is clear that the amount of titanium has the least effect on these three output parameters compared to other ones. According to the experimental results, it was observed that with increasing the amount of both the relative density and the theoretical density decrease. As mentioned in the previous sections, titanium has a low density so it does not have a significant effect on the density of the nanocomposite.

TABLE 6. Representation of the predicted apparent porosity, elastic, modules, hardness, relative density and theoretical density

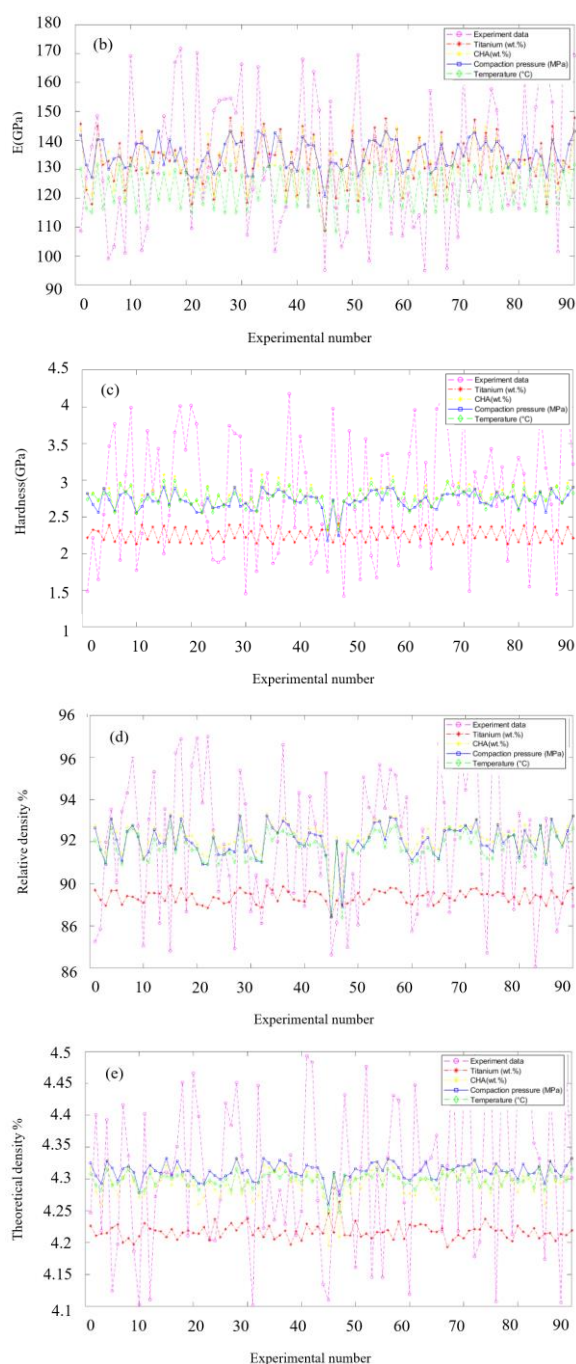| Output Dada obtain by GEP model	
Apparent porosity, %	6.05-9.01
E (GPa)	108.6-143.13
Hardness (GPa)	2.34-3.07
Relative density (%)	88.51-93.32

Figure 4. The sensitivity analysis for all parameters, (a) Apparent porosity,(b)Elastic modules, (c) Hardness, (d) Relative density, (e) Theoretical density

5. CONCLUSION

In this research, nanocomposite was produced by mechanical alloying method. After the experimental calculation of apparent porosity, elastic modulus, hardness, relative density and theoretical density as output parameters, GEP modeling was used to estimate

the effect of Ti and CHA wt.%, temperature and pressure on nanocomposite properties. Modeling was performed for each of the outputs and the model with the least error was selected for each of them (GEP-1 to GEP-5). For outputs that include porosity, elastic modulus, hardness, relative density, theoretical density. R^2 was obtained for testing ($R^2 = 0.9932, 0.9925, 0.9968, 0.9965, 0.9935$) and training ($R^2 = 0.9965, 0.9941, 0.9919, 0.9949, 0.9932$), respectively. For these 5 models, R is close to one and the values of MSE and RRSE are close to zero. These results show that Jeep modeling is a very accurate method for predicting the behavior of this nanocomposite. Finally, to be sure, sensitivity analysis was used to investigate the effect of input parameters on each of the output parameters. It was observed that the percentage by weight of Ti has the greatest effect on porosity, sintering temperature has the least effect on the elastic modulus and the percentage by weight of titanium has the least effect on the three outputs of hardness, relative density and theoretical density.

6. REFFERENCES

1. Rahmati, R. and Khodabakhshi, F., "Microstructural evolution and mechanical properties of a friction-stir processed ti-hydroxyapatite (ha) nanocomposite", *Journal of the Mechanical Behavior of Biomedical Materials*, Vol. 88, No., (2018), 127-139. https://doi.org/10.1016/j.jmbbm.2018.08.025

2. Okamoto, M. and John, B., "Synthetic biopolymer nanocomposites for tissue engineering scaffolds", *Progress in Polymer Science*, Vol. 38, No. 10-11, (2013), 1487-1503. https://doi.org/10.1016/j.progpolymsci.2013.06.001

3. Takallu, S., Mirzaei, E., Azadi, A., Karimizade, A. and Tavakol, S., "Plate-shape carbonated hydroxyapatite/collagen nanocomposite hydrogel via in situ mineralization of hydroxyapatite concurrent with gelation of collagen at ph= 7.4 and 37° c", *Journal of Biomedical Materials Research Part B: Applied Biomaterials*, Vol. 107, No. 6, (2019), 1920-1929. https://doi.org/10.1002/jbm.b.34284

4. Bovand, D., Yousefpour, M., Rasouli, S., Bagherifard, S., Bovand, N. and Tamayol, A., "Characterization of ti-ha composite fabricated by mechanical alloying", *Materials & Design (1980-2015)*, Vol. 65, No., (2015), 447-453. https://doi.org/10.1016/j.matdes.2014.09.021

5. Refaat, A., Youness, R.A., Taha, M.A. and Ibrahim, M., "Effect of zinc oxide on the electronic properties of carbonated hydroxyapatite", *Journal of Molecular Structure*, Vol. 1147, No., (2017), 148-154. https://doi.org/10.1016/j.molstruc.2017.06.091

6. Prasanna, A. and Venkatasubbu, G.D., "Sustained release of amoxicillin from hydroxyapatite nanocomposite for bone infections", *Progress in Biomaterials*, Vol. 7, No. 4, (2018), 289-296. https://doi.org/10.1007/s40204-018-0103-4

7. Hannora, A.E. and Ataya, S., "Structure and compression strength of hydroxyapatite/titania nanocomposites formed by high energy ball milling", *Journal of Alloys and Compounds*, Vol. 658, No., (2016), 222-233. https://doi.org/10.1016/j.jallcom.2015.10.240

8. Cao, Y., Shi, T., Jiao, C., Liang, H., Chen, R., Tian, Z., Zou, A., Yang, Y., Wei, Z. and Wang, C., "Fabrication and properties of zirconia/hydroxyapatite composite scaffold based on digital light

processing", *Ceramics International*, Vol. 46, No. 2, (2020), 2300-2308. https://doi.org/10.1016/j.ceramint.2019.09.219

9. Kwon, K.-A., Juhasz, J.A., Brooks, R.A. and Best, S.M., "Bioactive conformable hydrogel-carbonated hydroxyapatite nanocomposite coatings on ti-6al-4v substrates", *Materials Technology*, Vol. 35, No. 11-12, (2020), 727-733. https://doi.org/10.1080/10667857.2018.1475143

10. Youness, R.A., Taha, M.A., El-Kheshen, A.A. and Ibrahim, M., "Influence of the addition of carbonated hydroxyapatite and selenium dioxide on mechanical properties and in vitro bioactivity of borosilicate inert glass", *Ceramics International*, Vol. 44, No. 17, (2018), 20677-20685. https://doi.org/10.1016/j.ceramint.2018.08.061

11. Ahmed, M., Mansour, S., Al-Wafi, R., Afifi, M. and Uskoković, V., "Gold as a dopant in selenium-containing carbonated hydroxyapatite fillers of nanofibrous ε-polycaprolactone scaffolds for tissue engineering", *International Journal of Pharmaceutics*, Vol. 577, (2020), 118950. https://doi.org/10.1016/j.ijpharm.2019.118950

12. Niespodziana, K., "Synthesis and properties of porous ti-20 wt.% ha nanocomposites", *Journal of Materials Engineering and Performance*, Vol. 28, No. 4, (2019), 2245-2255. https://link.springer.com/article/10.1007/s11665-019-03966-8

13. Theingi, M., Tun, K.T. and Aung, N.N., "Preparation, characterization and optical property of lafeo3 nanoparticles via sol-gel combustion method", *SciMedicine Journal*, Vol. 1, No. 3, (2019), 151-157. https://doi.org/10.28991/SciMedJ-2019-0103-5

14. Gharibshahian, E., "The effect of polyvinyl alcohol concentration on the growth kinetics of ktiopo4 nanoparticles synthesized by the co-precipitation method", *HighTech and Innovation Journal*, Vol. 1, No. 4, (2020), 187-193. https://doi.org/10.28991/HIJ-2020-01-04-06

15. Gandomi, A.H., Alavi, A.H., Gandomi, M. and Kazemi, S., "Formulation of shear strength of slender rc beams using gene expression programming, part ii: With shear reinforcement", *Measurement*, Vol. 95, (2017), 367-376. https://doi.org/10.1016/j.measurement.2016.10.024

16. Abdellahi, M., Najafinezhad, A., Ghayour, H., Saber-Samandari, S. and Khandan, A., "Preparing diopside nanoparticle scaffolds via space holder method: Simulation of the compressive strength and porosity", *Journal of the Mechanical Behavior of Biomedical Materials*, Vol. 72, (2017), 171-181. https://doi.org/10.1016/j.jmbbm.2017.05.004

17. Trang, G.T.T., Linh, N., Linh, N. and Kien, P., "The study of dynamics heterogeneity in sio2 liquid", *HighTech and Innovation Journal*, Vol. 1, No. 1, (2020), 1-7. https://doi.org/10.28991/HIJ-2020-01-01-01

18. Ebrahimi-Kahrizsangi, R., Abdellahi, M. and Bahmanpour, M., "Ignition time of nanopowders during milling: A novel

simulation", *Powder Technology*, Vol. 272, (2015), 224-234. https://doi.org/10.1016/j.powtec.2014.12.009

19. Khayati, G.R., "A predictive model on size of silver nanoparticles prepared by green synthesis method using hybrid artificial neural network-particle swarm optimization algorithm", *Measurement*, Vol. 151, (2020), 107199. https://doi.org/10.1016/j.measurement.2019.107199

20. Ferreira, C., "Gene expression programming: A new adaptive algorithm for solving problems", arXiv preprint cs/0102027, (2001). https://arxiv.org/abs/cs/0102027

21. Sattari, R. and Khayati, G.R., "Prediction of the size of silver nanoparticles prepared via green synthesis: A gene expression programming approach", *Scientia Iranica*, Vol. 27, No. 6, (2020), 3399-3411. https://dx.doi.org/10.24200/sci.2020.53209.3112

22. Ghayour, H., Abdellahi, M. and Bahmanpour, M., "Artificial intelligence and ceramic tools: Experimental study, modeling and optimizing", *Ceramics International*, Vol. 41, No. 10, (2015), 13470-13479. https://doi.org/10.1016/j.ceramint.2015.07.1387

23. Abdellahi, M., Bahmanpour, H. and Bahmanpour, M., "The best conditions for minimizing the synthesis time of nanocomposites during high energy ball milling: Modeling and optimizing", *Ceramics International*, Vol. 40, No. 7, (2014), 9675-9692. https://doi.org/10.1016/j.ceramint.2014.02.049

24. Sabouhi, R., Ghayour, H., Abdellahi, M. and Bahmanpour, M., "Measuring the mechanical properties of polymer–carbon nanotube composites by artificial intelligence", *International Journal of Damage Mechanics*, Vol. 25, No. 4, (2016), 538-556. https://doi.org/10.1177%2F1056789515604375

25. Ebrahimi-Kahrizsangi, R., Abdellahi, M. and Bahmanpour, M., "Self-ignited synthesis of nanocomposite powders induced by spex mills; modeling and optimizing", *Ceramics International*, Vol. 41, No. 2, (2015), 3137-3151. https://doi.org/10.1016/j.ceramint.2014.10.158

26. Gholampour, A., Gandomi, A.H. and Ozbakkaloglu, T., "New formulations for mechanical properties of recycled aggregate concrete using gene expression programming", *Construction and Building Materials*, Vol. 130, (2017), 122-145. https://doi.org/10.1016/j.conbuildmat.2016.10.114

27. Jafari, M.M. and Khayati, G.R., "Prediction of hydroxyapatite crystallite size prepared by sol–gel route: Gene expression programming approach", *Journal of Sol-Gel Science and Technology*, Vol. 86, No. 1, (2018), 112-125. https://link.springer.com/article/10.1007/s10971-018-4601-6

28. Kök, M., Kanca, E. and Eyercioğlu, Ö., "Prediction of surface roughness in abrasive waterjet machining of particle reinforced mmcs using genetic expression programming", *The International Journal of Advanced Manufacturing Technology*, Vol. 55, No. 9, (2011), 955-968. https://link.springer.com/article/10.1007%252Fs00170-010-3122-4

Persian Abstract

<div dir="rtl">

چکیده

نانوبیوکامپوزیت‌های هیدروکسی آپاتیت کربنات- تیتانیوم به دلیل زیست‌سازگاری فوق‌العاده و خصوصیات مشابه آپاتیت استخوان، کاربردهای بیولوژیکی بسیاری مانند بیو ایمپلنت دارند. کربنات هیدروکسی آپاتیت از ویژگی‌های بیولوژیکی خوبی برخوردار است اما بزرگ‌ترین مشکل نانوکامپوزیت‌های Ti-CHA ویژگی‌های مکانیکی آنها مانند سختی، مدول یانگ، تخلخل ظاهری و تراکم نسبی است. پژوهش حاضر، با استفاده از برنامه نویسی بیان ژن (GEP)یک مدل پیش بینی می‌شود. از GEP برای بهینه سازی تأثیر فشار پرس، CHA و Ti و دمای تف‌جوشی بر خواص مکانیکی کنترل شده آنها استفاده می‌شود. برای دستیابی به این هدف 90 آزمایش مختلف برای ایجاد مدل‌های GEP در نظر گرفته شد. پس از آن نتایج به طور تصادفی به 63 مجموعه آموزش و 27 مجموعه آزمون تقسیم شدند. سرانجام 5 مورد از بهترین مدل‌ها برای هر پارامتر خروجی گزارش شدند. آنالیز حساسیت برای بررسی تاثیر پارامترهای عملی بر روی هر یک از خصوصیات کامپوزیت مانند سختی، مدول یانگ، تخلخل ظاهری و چگالی نسبی انجام شد. با مقایسه نتایج مطابقت قابل قبولی بین پارامترهای خروجی تجربی و پارامترهای به دست آمده از مدل GEP و آنالیز حساسیت مشاهده شد.

</div>